S1A

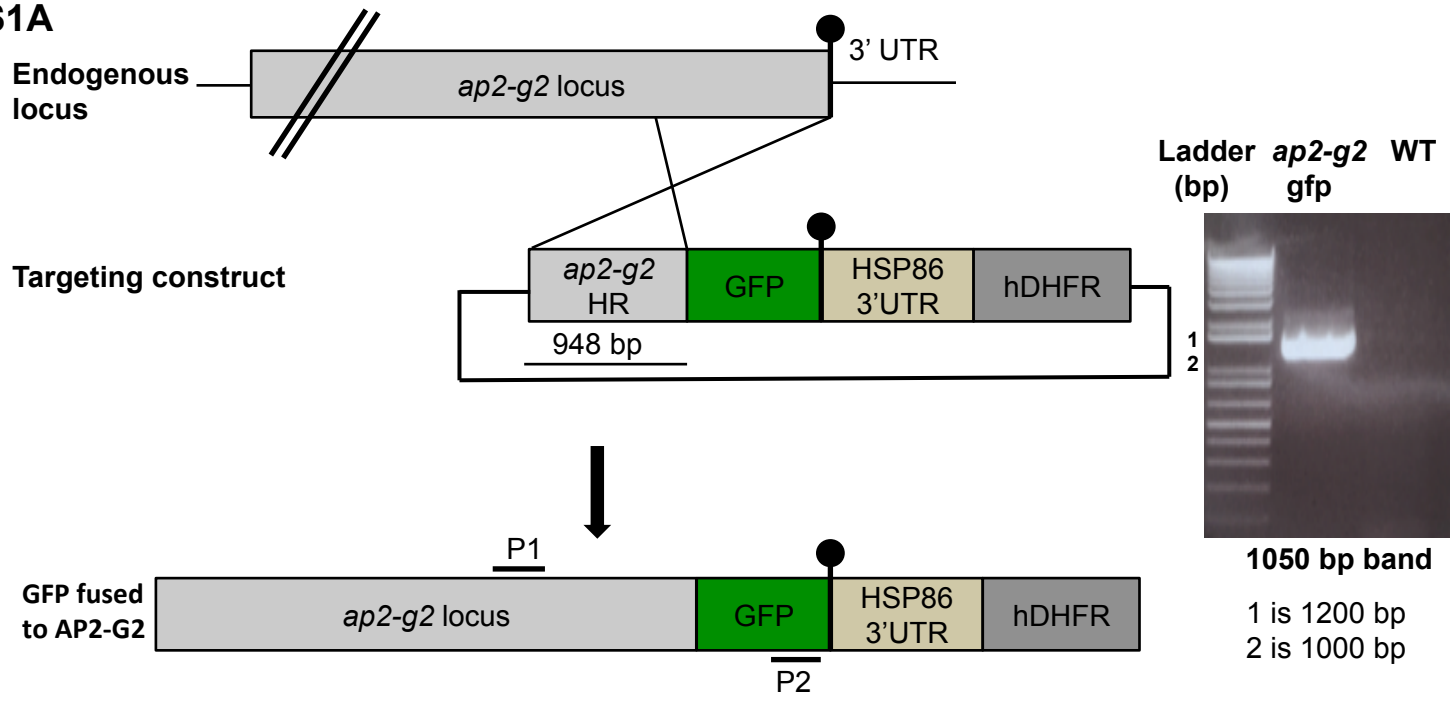

Supplementary Figure 1A Schematic showing the strategy used to tag the 3' end of the *pfap2-g2* gene with *gfp*. The tagged parasites were PCR-verified using the primers P1 and P2. A band of the right size was detected only in the transgenic parasite, suggesting the correct modification of the locus.

S1B

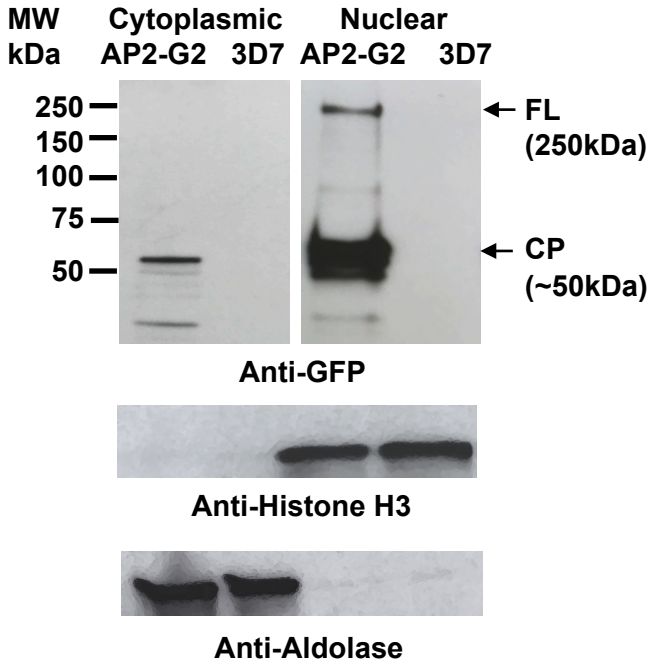

Supplementary Figure 1B Nuclear and cytoplasmic fractions from the GFP tagged PfAP2-G2 synchronized trophozoite stage parasites were subjected to western blot analysis using anti-GFP antibodies (1:1000). Full length (FL) GFP-tagged PfAP2-G2 (~250 kDa) was detected only in the nuclear fraction of the parasite lysate whereas cleavage product (CP, ~50kDa) was in both fractions. WT parasites were used as a negative control. Anti-histone H3 (1:3000) and anti-aldolase (1:1000) were used as loading controls for the nuclear and cytoplasmic fractions, respectively.

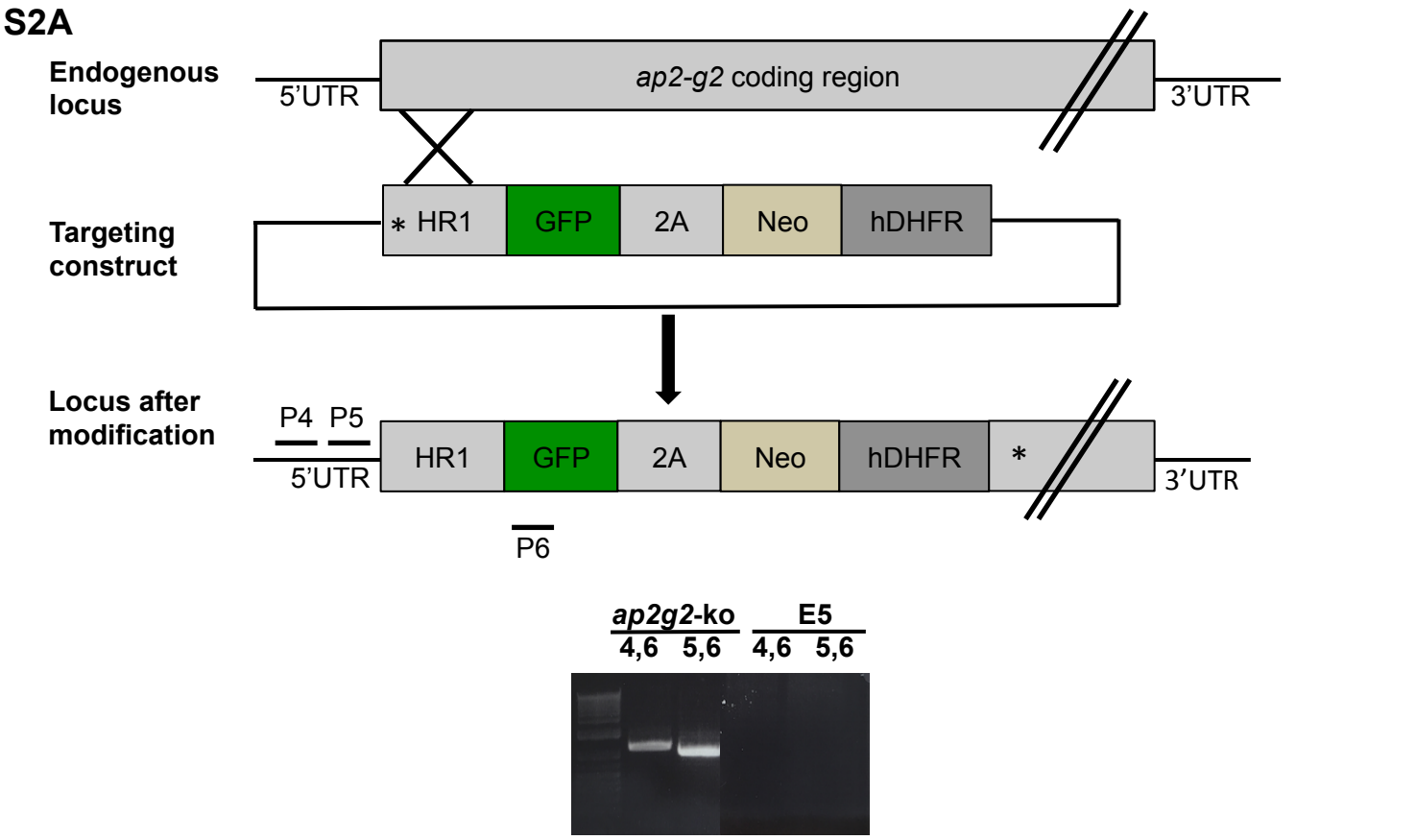

Supplementary Figure 2 (A) Schematic showing the strategy used to create the *pfap2-g2* knockout line using the selection linked integration (SLI) method (Birnbaum *et al*., 2017). A 500 bp homology region with the stop codon (starred) at the beginning ensured that the downstream fragment generated after the single homologous recombination was not expressed. The KO parasite was cloned by limiting dilution and was PCR-verified using the primers P4, P5 and P6. P4 and P5 binds to the 5' UTR upstream of the homology region, whereas primer P6 binds to the GFP, which can generate bands only in recombinant parasites and not in WT. (B) Live fluorescence imaging of the recombinant parasites expressing GFP with a disrupted *ap2-g2* locus in the mixed trophozoite and schizont stages. Image in the left shows that most of the parasites obtained were recombinant and the image in right confirms that stain is diffused throughout the parasites, suggesting that the protein is no longer localized in the nucleus.

S3

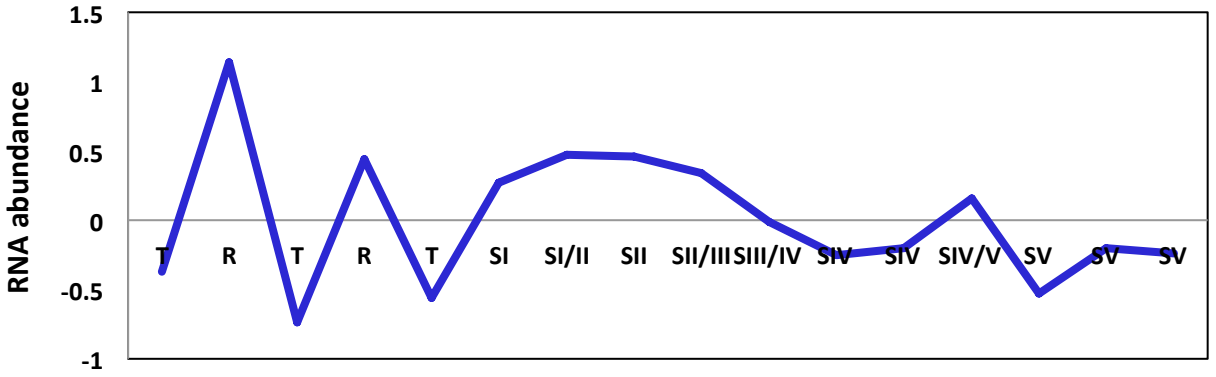

Supplementary Figure 3 Graph showing Transcriptional profile of *pfap2-g2* in asexual and gametocyte stages based on the previous research (van Biljon *et al.*, 2019). T is trophozite, R is ring and SI to SV is stage I to stage V of gametocytes.

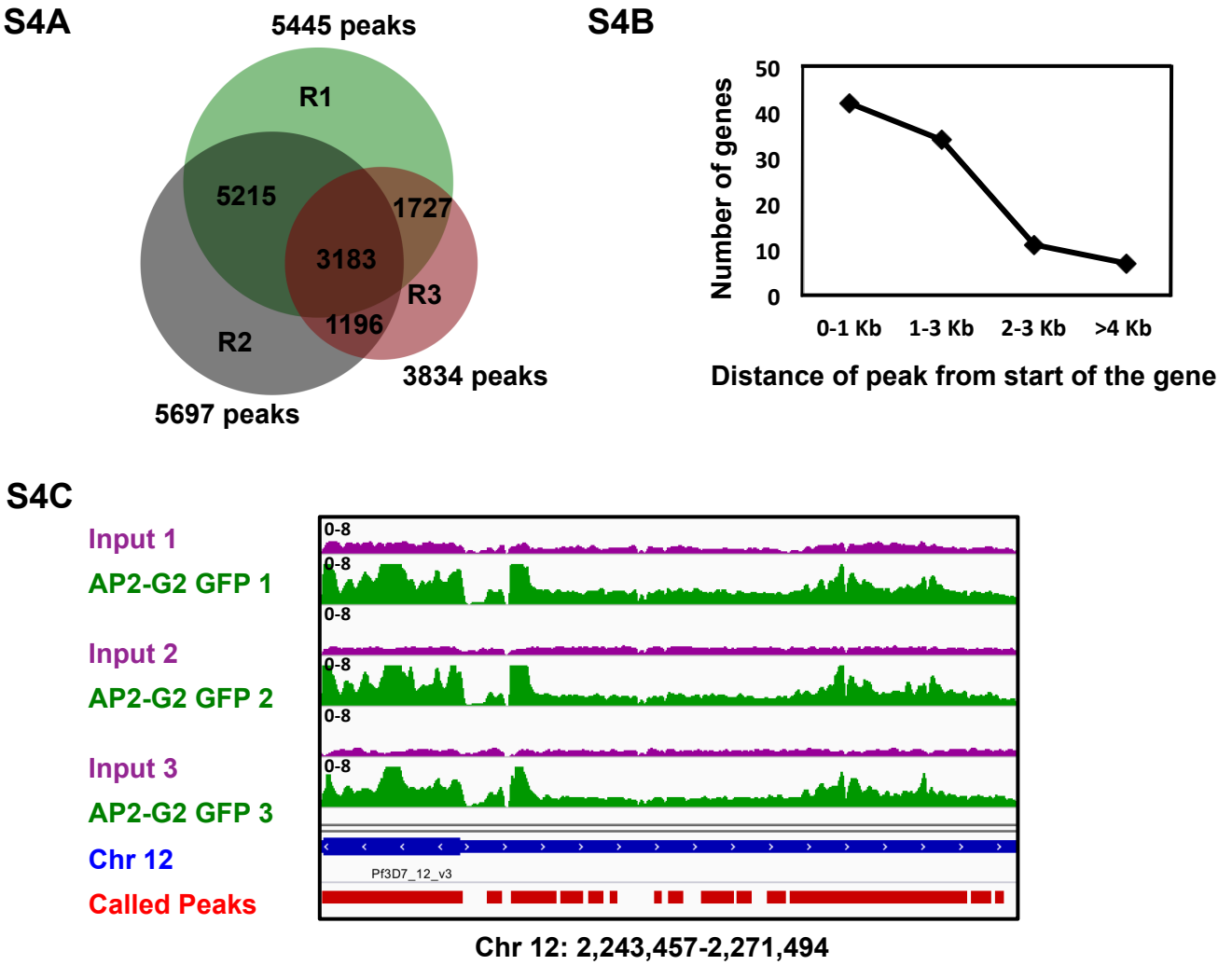

Supplementary Figure 4 (A) Peaks common in three replicates of ChIP-seq performed on PfAP2-G2 tagged with GFP using anti-GFP antibodies in trophozoite stage. (B) Graph showing distance of peaks from the start of the gene. 87% of PfAP2-G2 bound genes had peaks located within 2.5 Kb from the ATG of the gene. (C) Regions occupied by PfAP2-G2 at the end of chromosome XII in all three replicates. Thick blue tracks represent the chromosome and red tracks represent the called peaks by MACS2.

S5

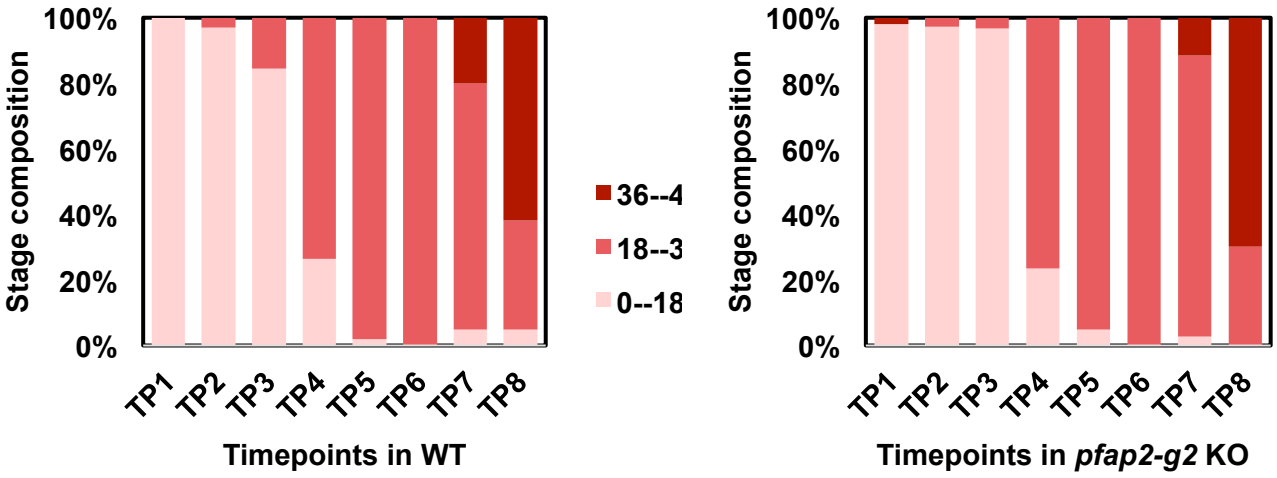

Supplementary Figure 5 Shown are the parasite counts from the DNA microarray timepoints (TP1 – TP8) in asexual stages in WT (wild-type) and *pfap2-g2* KO.

S6A

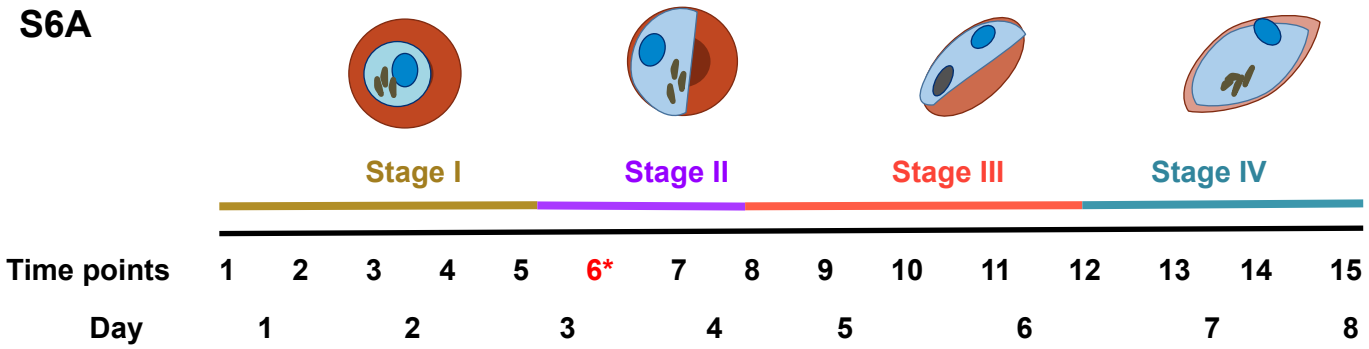

Supplementary Figure 6A Schematic showing mRNA collection time-points for gametocyte time course. Gametocyte induction was performed when the ring parasitemia was around 7-10%. The next cycle rings were set as day 1 of gametocytogenesis as some are sexually committed rings. To prevent reinvasion in the next cycle and thus formation of new asexuals, parasites were treated with 20U/ml heparin from day 1 post-induction through day 4. RNA was collected every 12 hours from day 1 to day 14 (stage I to stage IV).

***No data for TP6 due to technical reasons**

S6B

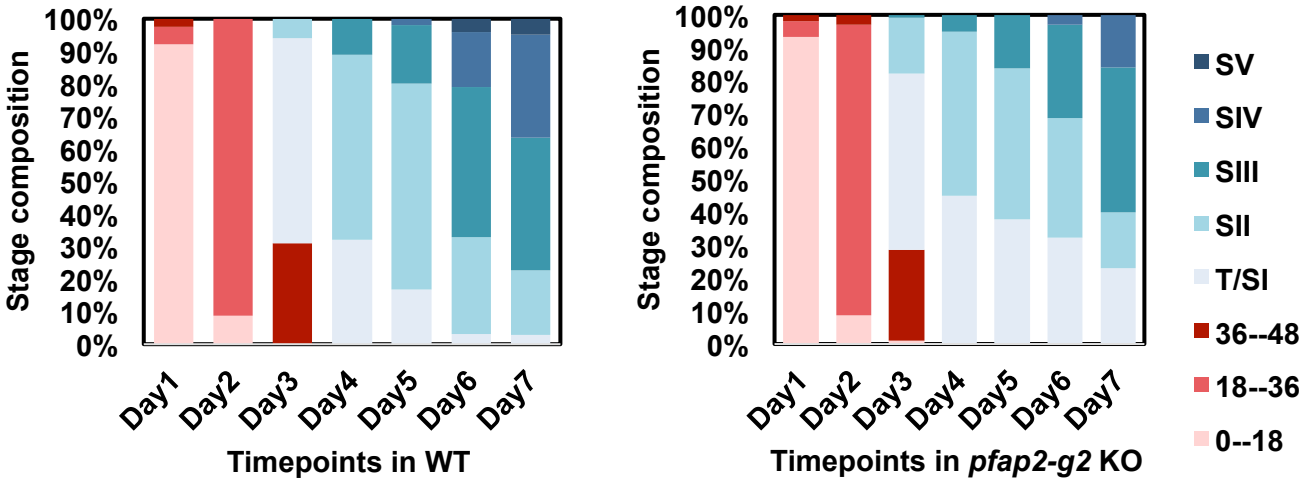

Supplementary Figure 6B Shown are the parasite counts from the microarray timepoints from day 1 through day 7 in gametocyte stages in WT (wild-type) and *pfap2-g2* KO.

S7

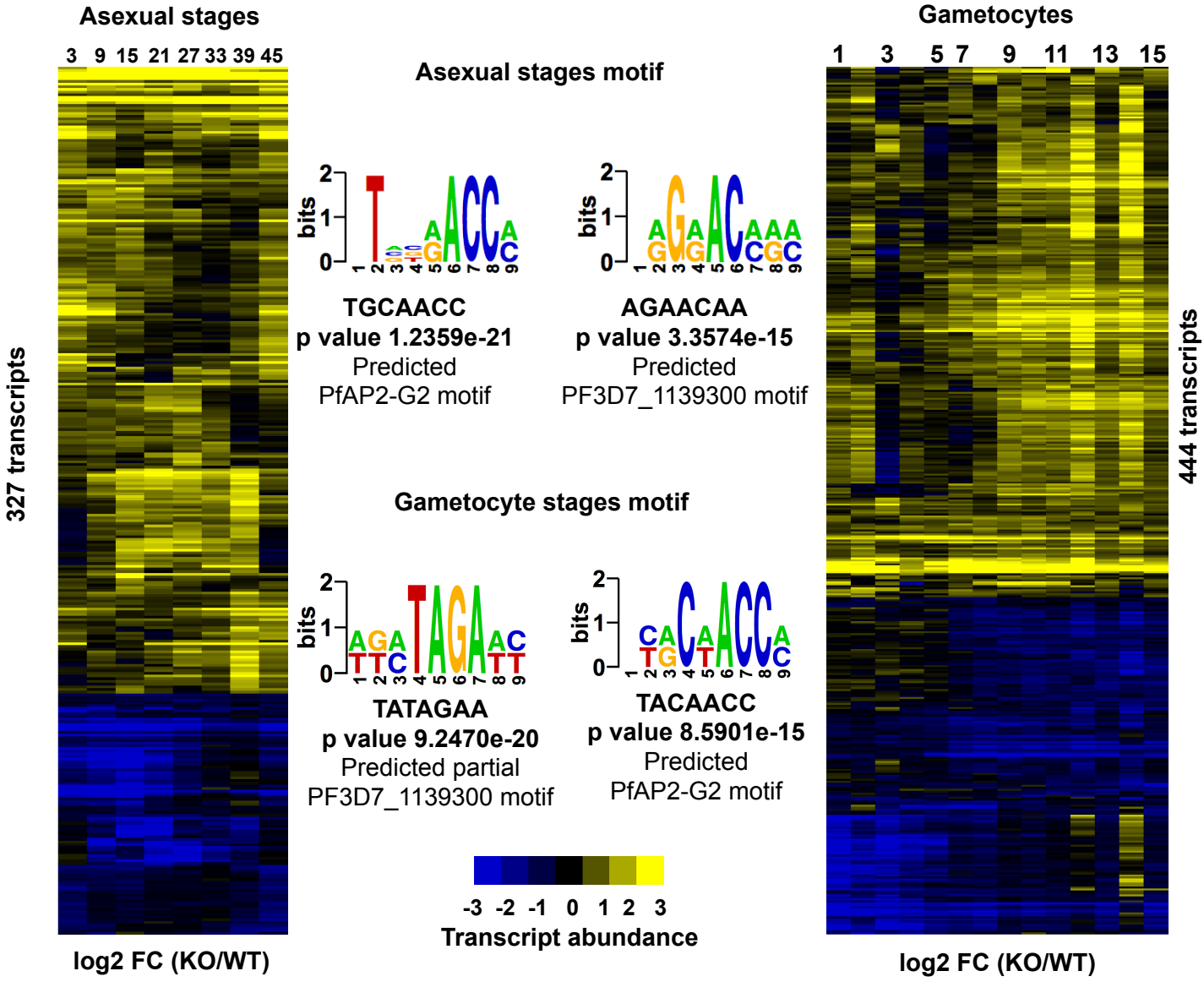

Supplementary Figure 7 Shown here are the heatmaps of the significantly changing transcripts in the PfAP2-G2 KO line compared to WT (>1.5 log2FC, 0.30 FDR) for both asexuals and gametocytes. Also, shown are the DNA sequence motif associated with the 5' upstream region of (~1000bp from the ATG) for genes with increased transcript abundance in asexual stage using finding informative regulatory elements (FIRE) algorithm. We also recover similar motif from the genes with increased and decreased transcript abundance in gametocytes.

S8

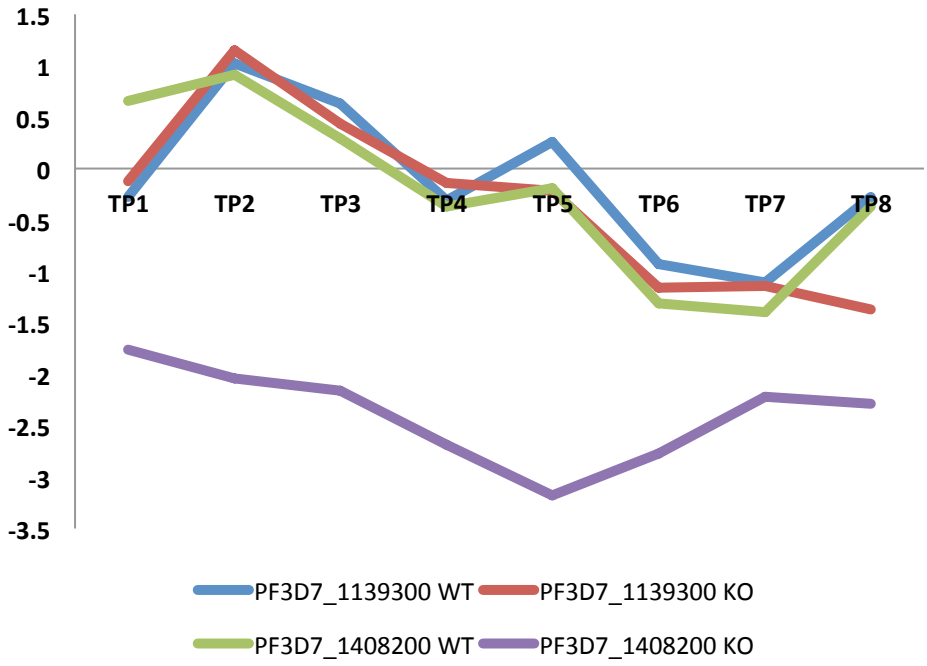

Supplementary Figure 8 Plot showing mRNA Expression level of PfAP2-G2 (PF3D7_1408200) and PF3D7_1139300 suggests that both are co-expressed.

S9

ATACATG
p value 4.3152e-10

TGTATTC
p value 1.2359e-12

TGTATTC
p value 4.5709e-08

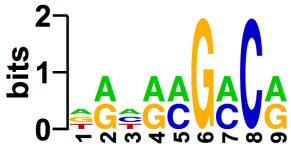

AAAAGAC
p value 4.4668e-12
Predicted partial Motif associated with gametocyte genes

Supplementary Figure 9 Shown are the DNA sequence motif associated with the 5' upstream region of (~1000bp from the ATG) for genes with decreased transcript abundance in asexual and gametocyte stages using finding informative regulatory elements (FIRE) algorithm.

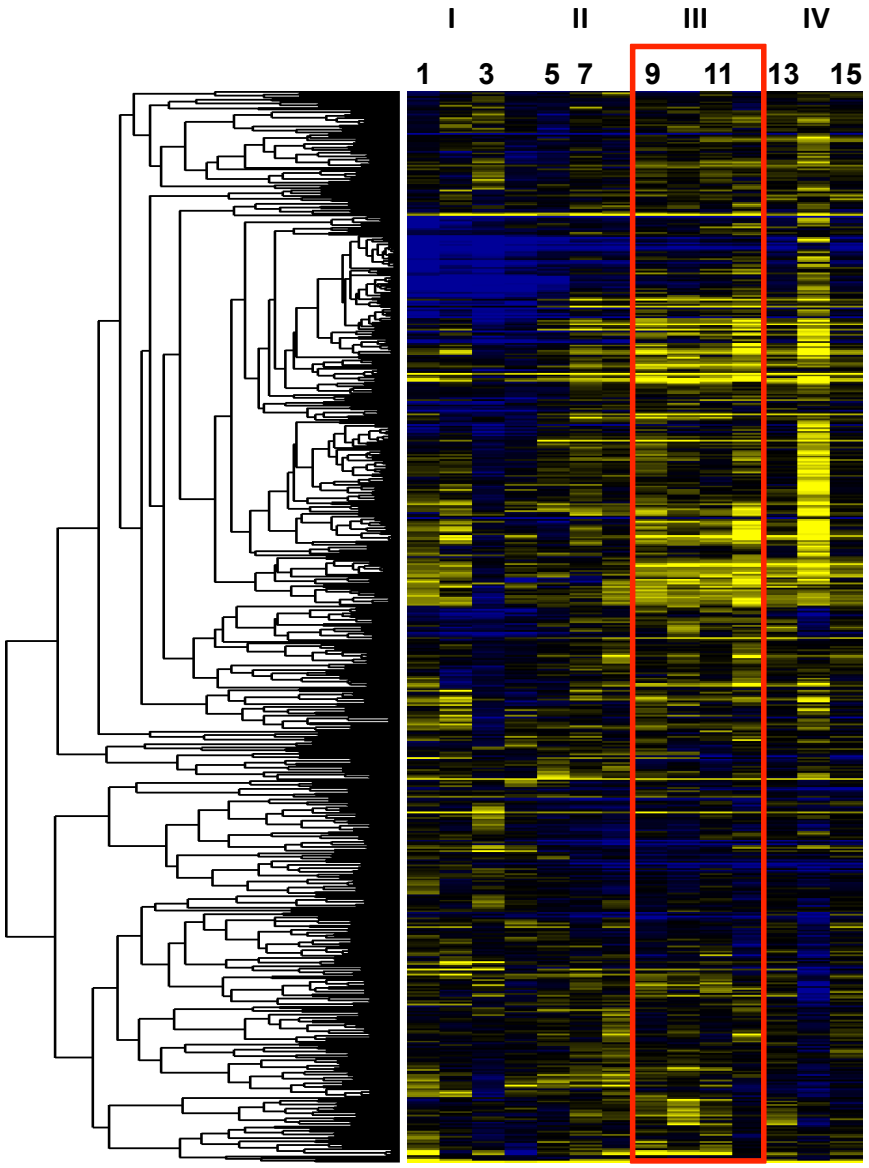

Supplementary Figure 10 Expression fold change (log2 KO versus WT) for the genes that are bound by PfAP2-G2 in the in the gene body in the gametocyte stage III. The genes are clustered based on Pearson's correlation. Boxed is the timepoint at which ChIP-seq was performed.

S11A

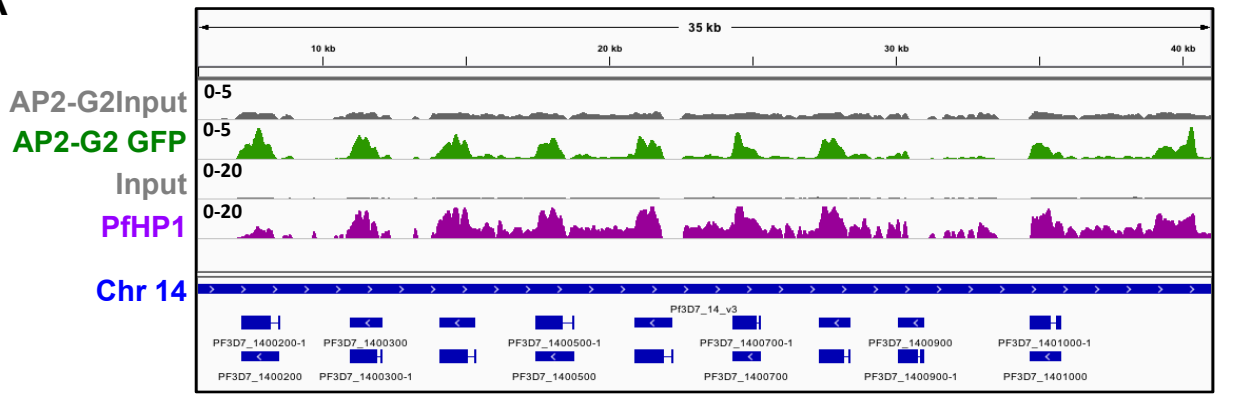

Pf3D7_14_v3:6,100-46,256

S11B

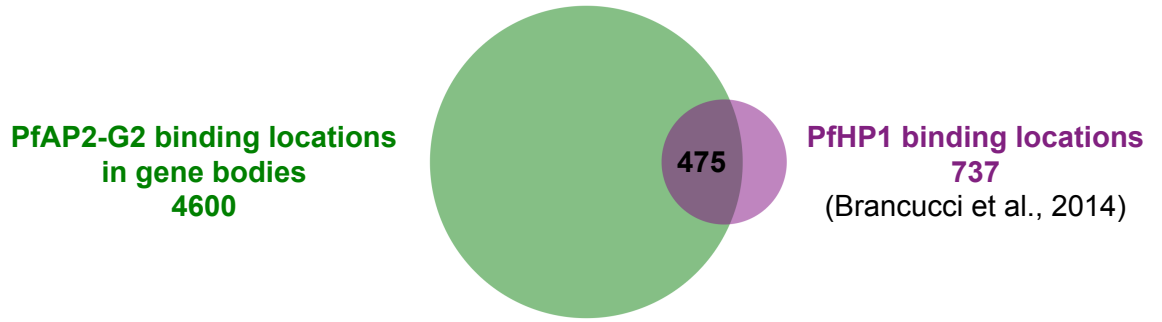

Supplementary Figure 11 PfAP2-G2 shows high correlation with H3K36me3 repressive histone modifications (A) IGV screenshot showing co-occupancy of PfAP2-G2 with PfHP1. First gray track represents Input for PfAP2-G2 and second green track shows the regions bound by PfAP2-G2. Third gray track represents input for PfHP1 and the last two pink tracks represent the regions bound by PfHP1 as indicated in the figure. Blue track shows the genes. (B) Venn diagram comparing the peaks obtained by ChIP-seq on PfHP1 marks (pink) (Brancucci *et al*., 2014) and PfAP2-G2-GFP (green) shows that 80% of times PfAP2-G2 shows co-occupancy with H3K36me3 marks.

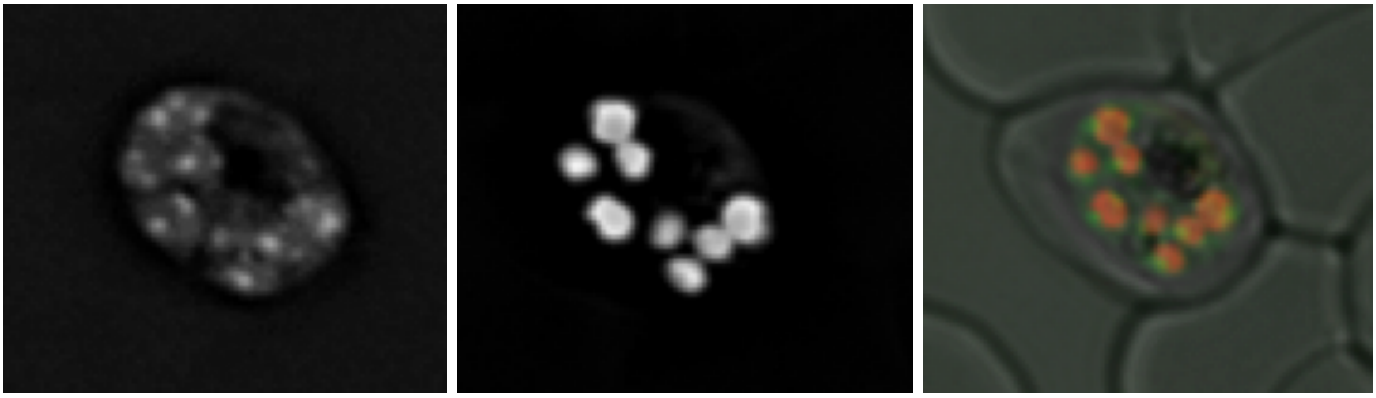

GFP Nucleus Merge

Supplementary Figure 12 PfAP2-G2 perinuclear localization in the schizont stages.

Supplementary Information

Supplementary Table 1: PfAP2-G2::GFP ChIP-seq data at the trophozoite stage The first tab of the table contains all of the upstream peaks common in two out of three biological replicates. The second tab has only 86 genes that were considered for further analysis. Indicated are the coordinates of each peak, the orientation of the gene, genes downstream to the peaks and distance between the peak and ATG start for each gene.

Supplementary Table 2: PfAP2-G2::GFP ChIP-seq data at the trophozoite stage The table contains peaks within gene-bodies common in two out of three biological replicates. Coordinates for each peak and the genes containing the peaks are indicated.

Supplementary Table 3: Comparison between the PfAP2-G2 and PbAP2-G2 ChIP-seq targets (Yuda *et al*. 2015) The first tab is the comparison of PbAP2-G2 upstream ChIP-seq target genes reported by Yuda *et. al*. compared to the PbAP2-G2 target genes we obtained using our ChIP-seq data analysis pipeline with the same parameters used in this study. The second tab is the same list of PbAP2-G2 upstream target genes, their orthologues in *P. falciparum*, and the PfAP2-G2 upstream targets we found in our trophozoite ChIP-seq data. The third tab is again the same list of PbAP2-G2 upstream target genes, their orthologues in *P. falciparum*, and the PfAP2-G2 upstream targets we found in our gametocyte ChIP-seq data. The fourth tab is the comparison of PbAP2-G2 targets in gene bodies we obtained using our ChIP-seq data analysis pipeline with the same parameters used in this study, their orthologues in *P. falciparum*, and the PfAP2-G2 targets in gene bodies we found in our trophozoite ChIP-seq data. (No gene body ChIP-seq targets were reported by Yuda *et al*.) The fifth tab is the same list of PbAP2-G2 gene-body targets, their orthologues in *P. falciparum*, and the PfAP2-G2 gene-body targets we found in our gametocyte ChIP-seq data.

Supplementary Table 4: PfAP2-G2::GFP ChIP-seq data in stage III gametocyte The table contains all of the upstream peaks common in two biological replicates. Indicated are the coordinates of each peak, the orientation of the gene, genes downstream to the peaks and distance between the peak and ATG start for each gene.

Supplementary Table 5: PfAP2-G2::GFP ChIP-seq data in stage III gametocyte The table contains peaks within gene bodies common in two biological replicates. Coordinates for each peak and the genes containing the peaks are indicated.

Supplementary Table 6: List of the differentially expressed genes (*pfap2-g2* KO vs. WT) in asexual blood stages Significance analysis of microarray (SAM) of the asexual stage timecourse data found that 327 transcripts were differentially expressed (>1.5 log2FC, 0.30 local FDR) in the ***pfap2-g2*** KO line compared to WT. Out of these, 237 showed enhanced transcript abundance in the ***pfap2-g2*** KO line and 90 showed decreased abundance. The first tab has upregulated genes and the second tab has downregulated genes along with fold change, q-value and the local false discovery rate.

Supplementary Table 7: List of the differentially expressed genes (*pfap2-g2* KO vs. WT) in gametocytes Significance analysis of microarray (SAM) of the gametocyte timecourse data found that 444 transcripts were differentially expressed (>1.5 log2FC, 0.30 local FDR) in the ***pfap2-g2*** **KO** line compared to WT. Out of these, 274 showed enhanced transcript abundance in the ***pfap2-g2*** **KO** line and 170 showed decreased abundance. The first tab has upregulated genes and the second tab has downregulated genes along with fold change, q value and the local false discovery rate.

Supplementary Table 8: List of PfAP2-G2 interacting partners The first tab contains the list of peptides obtained in the upper band of the PfAP2-G2-GFP IP (**Figure 7A**) and the second tab has the list of peptides obtained in the lower band of PfAP2-G2-GFP IP gel (**Figure 7A**) along with the spectral counts, average and maximum probability and FDR. Only proteins with high probability of interaction as measured by SAINT (pSAINT 0.9 and 1%FDR) were considered for the analysis.

Supplementary Table 9: List of all primers used to create and verify the genetically modified parasite lines.